

EMBEDDED DISCONTINUITIES FOR SOFTENING SOLIDS

G.N. Wells¹ and L.J. Sluys²

¹Faculty of Aerospace Engineering

²Faculty of Civil Engineering and Geosciences

Koiter Institute Delft / Delft University of Technology

P.O. Box 5048, 2600 GA Delft, The Netherlands

ABSTRACT

Additional, discontinuous functions are added to the displacement field of standard finite elements in order to capture highly localised zones of intense straining. By embedding discontinuities within an element it is possible to effectively model localisation phenomena (such as fracture in concrete) with a relatively small number of finite elements. The displacement jump is regularised, producing bounded strains and allowing the application of classical strain softening constitutive laws. It is then possible to achieve mesh-objective results with respect to energy dissipation without resorting to higher-order continuum theories.

KEYWORDS

Localisation, embedded discontinuity, strong discontinuity, enhanced strain, fracture, softening, damage, plasticity.

INTRODUCTION

Recently, attention has been paid to so-called ‘embedded discontinuity’ models as a means to overcome the limitations of smeared and discrete crack models. By capturing a crack within an element, it is effectively possible to model a discrete phenomenon within a continuum framework. Embedded discontinuities offer a hybrid approach between smeared and discrete modelling.

The deficiency of discrete crack models is the dependence on mesh alignment, when separation can occur only at elements interfaces. To remedy this, special, computer intensive

re-meshing techniques are required. The weakness of smeared crack models is their inherent dependency on element size and alignment (Rots, 1988). Attempts to overcome element size dependency through simple fracture energy regularisation are only partly successful, as this method provides no information over crack direction nor is the necessary length scale (so-called crack bandwidth) mesh objective. By embedding a discontinuity, direction information is taken from stress or strain field and kinematic enhancements make elements more able to properly reproduce the real deformation modes.

The application of gradient (de Borst et al., 1993) and non-local (Pijaudier-Cabot & Bažant, 1987) continuum theories has proved successful in overcoming the deficiency of the classical continuum when analysing softening materials. However, the common feature of higher-order models is the need for a fine mesh within the localisation zone in order to capture the high strain gradients. This limits the potential of such methods for structural scale problems, especially in three-dimensions.

Embedded discontinuity models can be placed broadly in two classes, *weak* and *strong* discontinuities. Weak discontinuities involve the addition of discontinuous modes to the strain field while maintaining a continuous displacement field (Sluys & Berends, 1998). This approach avoids the need to deal with unbounded strains as a result of a displacement jump, but the ability of such models to reproduce full crack separation in mode-I type problems is questionable (Jirásek, 1998). The model developed here incorporates a *strong* discontinuity. The common feature of strong discontinuities is that a jump is added in the displacement field of a finite element (Oliver & Simo, 1994; Lotfi & Shing, 1995; Larsson & Runesson, 1996). The model developed here uses a specially constructed shape function to represent the deformations at the discontinuity in conjunction with a specially constructed interpolation function that is used in calculating the internal forces. This method is able to fully represent the kinematics of the problem as well as neatly satisfy traction continuity across the discontinuity.

STRONG DISCONTINUITY FORMULATION

Consider a body Ω that is crossed by a material discontinuity (Figure 1). The body is composed of two sub-domains, Ω^+ and Ω^- , that lie on either side of the discontinuity Γ_d . In addition, a *discontinuity band* (Ω^d), centred on Γ_d and a sub-domain of Ω , is also defined.

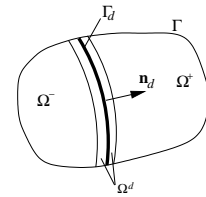


Figure 1: Body containing a discontinuity

Discontinuous displacement field

The displacement field of a body containing a discontinuity can be decomposed into two parts; a continuous ($\hat{\mathbf{u}}(\mathbf{x}, t)$) and a discontinuous ($\mathcal{H}_{\Gamma_d}[\mathbf{u}](\mathbf{x}, t)$) component. The jump in displacement is provided via the Heaviside function (\mathcal{H}_{Γ_d}), centred on the discontinuity, operating on a continuous function $[\mathbf{u}](\mathbf{x}, t)$. However, in the context of finite element implementation, this presents difficulties since both components must be taken into account when imposing essential boundary conditions. A more suitable approach is to specially develop

the decomposition such that the contribution of the discontinuous component is zero on the boundaries. Hence, only the regular, continuous part of the displacement field must be taken into account.

$$\mathbf{u}(\mathbf{x}, t) = \hat{\mathbf{u}}(\mathbf{x}, t) + (\mathcal{H}_{\Gamma_d} - \varphi(\mathbf{x}))[\tilde{\mathbf{u}}](\mathbf{x}, t) \quad (1)$$

In (1), $[\tilde{\mathbf{u}}](\mathbf{x}, t)$ is the magnitude of the discrete displacement jump at the discontinuity and $\varphi(\mathbf{x})$ is a continuous function that satisfies

$$\varphi(\mathbf{x}) = \begin{cases} 1 & \text{in } \Omega^+ \setminus \Omega^d \\ 0 & \text{in } \Omega^- \setminus \Omega^d \end{cases} \quad (2)$$

The displacement decomposition is shown in Figure 2. The strain field can be easily found by calculating the gradient of (1).

$$\boldsymbol{\varepsilon}(\mathbf{x}, t) = \nabla^s \hat{\mathbf{u}} + ((\delta_{\Gamma_d} \mathbf{n}_d - \nabla^s \varphi) \otimes [\tilde{\mathbf{u}}]) \quad (3)$$

Note the appearance of the Dirac delta distribution (δ_{Γ}) in the strain expression. From the inclusion of a displacement jump, the strain field at the discontinuity is unbounded.

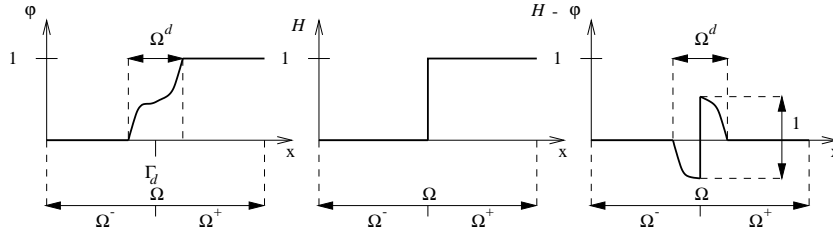


Figure 2: Displacement decomposition

Mixed variational formulation

To construct an element that incorporates a displacement discontinuity, it is necessary to start from the variational formulation. It is useful to begin from a modified form of the three-field variational statements that includes so-called *enhanced strains* (Simo & Rifai, 1990). The strain field is decomposed into a compatible ($\nabla^s \mathbf{u}$) and incompatible ($\tilde{\boldsymbol{\varepsilon}}$) parts, yielding

$$\begin{aligned} \int_{\Omega} \nabla^s \boldsymbol{\eta} : \boldsymbol{\sigma}(\nabla^s \mathbf{u} + \tilde{\boldsymbol{\varepsilon}}) d\Omega - W^{ext}(\boldsymbol{\eta}) &= 0 \\ \int_{\Omega} \boldsymbol{\tau} : \tilde{\boldsymbol{\varepsilon}} d\Omega &= 0 \\ \int_{\Omega} \tilde{\boldsymbol{\gamma}} : (-\boldsymbol{\sigma} + \boldsymbol{\sigma}(\nabla^s \mathbf{u} + \tilde{\boldsymbol{\varepsilon}})) d\Omega &= 0 \end{aligned} \quad (4)$$

where $(\boldsymbol{\eta}, \boldsymbol{\gamma}, \boldsymbol{\tau}) \in (V \times E \times S)$ are all variations of displacements, strains and stresses respectively with $(V \times E \times S)$ the spaces of admissible displacement, strain and stress variations.

In order to allow for a strong discontinuity, (4) must be further modified by decomposing the enhanced strains into continuous ($\tilde{\boldsymbol{\varepsilon}}_c$) and a discontinuous ($\tilde{\boldsymbol{\varepsilon}}_d$) parts. Taking into account

that the discontinuous part of the enhanced strain field is non-zero only on Γ_d and using the divergence theorem, (4) can be re-phrased allowing for a displacement jump

$$\begin{aligned} \int_{\Omega} \nabla^s \boldsymbol{\eta} : \boldsymbol{\sigma}(\nabla^s \mathbf{u} + \tilde{\boldsymbol{\varepsilon}}) d\Omega - W^{ext}(\boldsymbol{\eta}) &= 0 \\ \int_{\Omega} \boldsymbol{\tau} : \tilde{\boldsymbol{\varepsilon}}_c d\Omega + \int_{\Gamma_d} (\boldsymbol{\tau} \boldsymbol{\nu}_d) \cdot \mathbf{n}_d d\Gamma &= 0 \\ \int_{\Omega} \tilde{\boldsymbol{\gamma}}_c : (-\boldsymbol{\sigma} + \boldsymbol{\sigma}(\nabla^s \mathbf{u} + \tilde{\boldsymbol{\varepsilon}})) d\Omega + \int_{\Gamma_d} [(-\boldsymbol{\sigma} + \boldsymbol{\sigma}(\nabla^s \mathbf{u} + \tilde{\boldsymbol{\varepsilon}})) \boldsymbol{\eta}_d] \cdot \mathbf{n}_d d\Gamma &= 0 \end{aligned} \quad (5)$$

where $\boldsymbol{\nu}_d$ is discrete displacement at the discontinuity and $\boldsymbol{\eta}_d$ is a variation of the discrete displacement at the discontinuity.

From this point, there have been two different approaches. The first is the *kinematic* approach, where extra discontinuous shape functions are added to the element (Lotfi & Shing, 1995). This method is kinematically representative of the real deformations and allows full separation at the interface, but leads to difficulties in imposing the traction continuity conditions in (5)_{2,3}. The alternative is to use *enhanced assumed strains* (EAS), where the enhanced modes are constructed in the strain space, orthogonal to the stress field, thereby automatically satisfying (5)₂ and eliminating the stresses from the unknown fields. This approach allows traction continuity across the discontinuity to be easily satisfied, although it is kinematically lacking with respect to the former approach.

The approach followed here is a hybrid between the kinematic and the EAS methods. The kinematic approach is used to enhance the kinematic fields, while the EAS approach is used in calculating the internal forces and hence impose the traction continuity (Oliver, 1996; Wells, 1999).

Finite element implementation

The discretised form of the displacement and strain fields including a discontinuity, for time-independent models, can be written as follows

$$\mathbf{u}(\mathbf{x}) = \mathbf{N}_a(\mathbf{x}) \mathbf{a}_e + \mathbf{N}_\alpha(\mathbf{x}) \boldsymbol{\alpha}_e \quad (6)$$

$$\boldsymbol{\varepsilon}(\mathbf{x}) = \mathbf{B}(\mathbf{x}) \mathbf{a}_e + \mathbf{G}(\mathbf{x}) \boldsymbol{\alpha}_e \quad (7)$$

where \mathbf{N}_a and \mathbf{B} are the normal displacement and strain interpolation matrices respectively, \mathbf{N}_α and \mathbf{G} (gradient of \mathbf{N}_α) collect the interpolation functions for the enhanced displacement and strain fields respectively, \mathbf{a}_e are the nodal displacements and $\boldsymbol{\alpha}_e$ are the displacements associated with the enhanced modes at the discontinuity. The matrix \mathbf{G} for an element can be constructed by examining the enhanced part of the kinematic strain field (3). In two-dimensions this gives

$$\mathbf{G}_e = \begin{bmatrix} \delta_{\Gamma_d} n_x - \frac{\partial \varphi(\mathbf{x})}{\partial x} & 0 \\ 0 & \delta_{\Gamma_d} n_y - \frac{\partial \varphi(\mathbf{x})}{\partial y} \\ \delta_{\Gamma_d} n_y - \frac{\partial \varphi(\mathbf{x})}{\partial y} & \delta_{\Gamma_d} n_x - \frac{\partial \varphi(\mathbf{x})}{\partial x} \end{bmatrix} \quad (8)$$

Next, attention must be paid to the traction continuity condition. The orthogonality condition (5)₂ means that (5)₃ can be rephrased as

$$\int_{\Omega} \tilde{\boldsymbol{\gamma}}_c : \boldsymbol{\sigma}(\nabla^s \mathbf{u} + \tilde{\boldsymbol{\varepsilon}}) d\Omega + \int_{\Gamma_d} (\boldsymbol{\sigma}(\nabla^s \mathbf{u} + \tilde{\boldsymbol{\varepsilon}}) \boldsymbol{\eta}_d) \cdot \mathbf{n}_d d\Gamma = 0 \quad (9)$$

Considering that (5)₂ must apply for each element gives

$$\int_{\Omega_e} \tilde{\boldsymbol{\gamma}} : \boldsymbol{\tau} \, d\Omega = \int_{\Omega_e \setminus \Gamma_d} \tilde{\boldsymbol{\gamma}}_c : \boldsymbol{\tau} \, d\Omega + \int_{\Gamma_{d,e}} (\boldsymbol{\tau} \boldsymbol{\eta}_d) \cdot \mathbf{n}_d \, d\Gamma = 0 \quad (10)$$

For a straight discontinuity (that is, \mathbf{n}_d is constant), a piecewise constant strain field and taking into account that in order to pass the patch test (Taylor et al., 1986), (10) must hold for an arbitrary constant stress field, (10) can be integrated explicitly.

$$A_e \tilde{\boldsymbol{\gamma}}_c = -l_e (\mathbf{n}_d \otimes \boldsymbol{\eta}_d) \quad (11)$$

Rearranging (11), an expression for the strain field outside the discontinuity can be found.

$$\tilde{\boldsymbol{\gamma}}_c = -\frac{l_e}{A_e} \mathbf{n}_d \otimes \boldsymbol{\eta}_d \quad (12)$$

For the two-dimensional case, l_e is the length of the discontinuity through the element and A_e is the area of the element. For the three-dimensional case, l_e is the area of the discontinuity plane through the element and A_e is the volume of the element.

Taking the traction continuity condition (9), which must also apply for each element, and now expressing $\boldsymbol{\sigma}(\nabla^s \mathbf{u} + \tilde{\boldsymbol{\varepsilon}})$ as $\boldsymbol{\sigma}(\boldsymbol{\varepsilon})$

$$\int_{\Omega_e} \tilde{\boldsymbol{\gamma}}_c : \boldsymbol{\sigma}(\boldsymbol{\varepsilon}) \, d\Omega + \int_{\Gamma_d} (\boldsymbol{\sigma}(\boldsymbol{\varepsilon}) \boldsymbol{\eta}_d) \cdot \mathbf{n}_d \, d\Gamma = 0 \quad (13)$$

Substituting the continuous part of the enhanced strain field (12) into (13)

$$\int_{\Omega_e \setminus \Gamma_d} \left(-\frac{l_e}{A_e} \mathbf{n}_d \otimes \boldsymbol{\eta}_d\right) : \boldsymbol{\sigma}(\boldsymbol{\varepsilon}) \, d\Omega + \int_{\Gamma_d} (\boldsymbol{\sigma}(\boldsymbol{\varepsilon}) \boldsymbol{\eta}_d) \cdot \mathbf{n}_d \, d\Gamma = 0 \quad (14)$$

Now using properties of the Dirac-delta distribution

$$\int_{\Omega_e \setminus \Gamma_d} \left(-\frac{l_e}{A_e} \mathbf{n}_d \otimes \boldsymbol{\eta}_d\right) : \boldsymbol{\sigma}(\boldsymbol{\varepsilon}) \, d\Omega + \int_{\Omega_e} \delta_{\Gamma_d} (\boldsymbol{\sigma}(\boldsymbol{\varepsilon}) \boldsymbol{\eta}_d) \cdot \mathbf{n}_d \, d\Omega = 0 \quad (15)$$

Equation (14) can be rearranged to express the traction force on the discontinuity and in the bulk of the element.

$$\underbrace{\frac{1}{A_e} \int_{\Omega_e \setminus \Gamma_{d,e}} \boldsymbol{\sigma}(\boldsymbol{\varepsilon}) \mathbf{n}_d \, d\Omega}_{\text{average on } \Omega_e \setminus \Gamma_d} = \underbrace{\frac{1}{l_e} \int_{\Gamma_{d,e}} \boldsymbol{\sigma}(\boldsymbol{\varepsilon}) \mathbf{n}_d \, d\Gamma}_{\text{average on } \Gamma_d} \quad (16)$$

For constant strain elements (three-noded triangle and four-noded tetrahedron), the constant strain field assumption used to find (12) is exact, so the average tractions (16) are also the exact solution. For higher order elements, the traction continuity requirement is imposed in an average sense.

For finite element implementation, it is necessary to form an interpolation matrix (\mathbf{G}^*) for calculating the internal force vector associated with the degree of freedom at the discontinuity.

$$\mathbf{f}^{int} = \int_{\Omega} \left\{ \begin{array}{c} \mathbf{B}^T \boldsymbol{\sigma} \\ \mathbf{G}^{*T} \boldsymbol{\sigma} \end{array} \right\} d\Omega = \left\{ \begin{array}{c} \mathbf{f}_u^{int} \\ \mathbf{f}_\alpha^{int} \end{array} \right\} \quad (17)$$

Taking variations of $\boldsymbol{\eta}_d$ in equation (15), a special interpolation matrix \mathbf{G}_e^* can be formed

$$\mathbf{G}_e^* = \left(\delta_{\Gamma_d} - \frac{l_e}{A_e} \right) \mathbf{n}_d \quad (18)$$

where for two-dimensional problems the, the matrix \mathbf{n}_d is

$$\mathbf{n}_d^T = \begin{bmatrix} n_x & 0 & n_y \\ 0 & n_y & n_x \end{bmatrix} \quad (19)$$

From the virtual work equation, the element stiffness matrix can then be formed

$$\int_{\Omega_e} \begin{bmatrix} \mathbf{B}_e^T \mathbf{D} \mathbf{B}_e & \mathbf{B}_e^T \mathbf{D} \mathbf{G}_e \\ \mathbf{G}_e^{*T} \mathbf{D} \mathbf{B}_e & \mathbf{G}_e^{*T} \mathbf{D} \mathbf{G}_e \end{bmatrix} d\Omega \begin{Bmatrix} \dot{\mathbf{a}}_e \\ \dot{\boldsymbol{\alpha}}_e \end{Bmatrix} = \begin{Bmatrix} \dot{\mathbf{f}}_{u,e}^{int} \\ \mathbf{0} \end{Bmatrix} \quad (20)$$

As with EAS methods, the enhanced, incompatible modes can be statically condensed at element level. This makes the method simple to implement in existing finite element codes. Notice that the hybrid approach, in general, results in a non-symmetric element stiffness matrix, irrespective of the constitutive model applied.

The final step to apply the method numerically is to deal with the Dirac-delta distribution. Since unbounded strains do not fit with numerical implementation, nor with continuum constitutive laws, the Dirac-delta distribution is regularised with a function that satisfies the necessary integration properties of the distribution.

$$\delta_{\Gamma} \approx \frac{1}{k} \quad (21)$$

As $k \rightarrow 0$, the approximation (21) approaches the exact solution.

NUMERICAL EXAMPLES

The following example has been analysed with the embedded discontinuity and smeared Rankine models for two unstructured meshes of different densities. The underlying element is a three-noded triangle and a Rankine plasticity constitutive law with exponential softening has been applied. The specimen is taken from Berends et al. (1997) and the material parameters are: $E = 10 \times 10^3 \text{MPa}$, $\nu = 0.2$, $f_{ct} = 1.0 \text{MPa}$, $G_f = 0.02 \text{N/mm}^2$ and $k = 1.0 \times 10^{-7} \text{mm}$. It can be seen in Figure 3 that the embedded model gives indistinguishable results for the two meshes, while conventional Rankine model with fracture energy regularisation gives a difference in total energy dissipation for the two meshes. The deformed meshes for the embedded analysis are also shown in Figure 3.

CONCLUSIONS

The embedment of discontinuities can be successfully applied to overcome mesh dependence in softening problems. It is also a promising technique to model curved cracking via classical

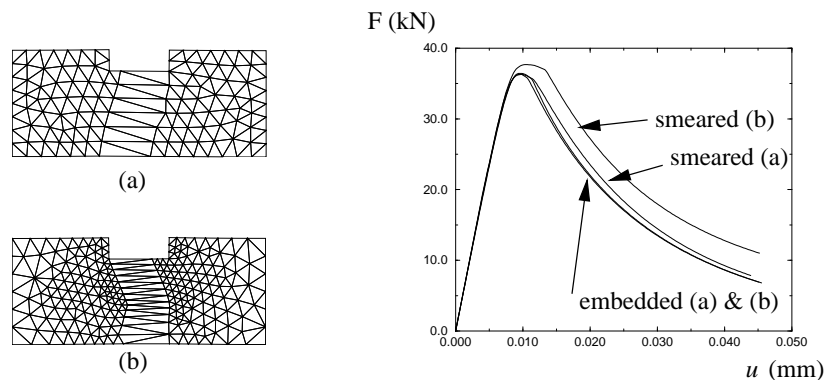


Figure 3: Load-displacement and deformed meshes (with rotating discontinuity)

continuum laws, which has not been successful using smeared approaches. Since the discontinuous modes are incompatible and continuum constitutive laws are applied, the method can be easily implemented in existing finite element codes. However, some care must still be taken when applying continuum relationships that spurious stress states do not develop (plasticity) and robustness is not severely compromised when calculating a consistent tangent (damage).

ACKNOWLEDGMENTS

This research is supported by the Technology Foundation STW, applied science division of NWO and the technology program of the Ministry of Economic Affairs, The Netherlands.

REFERENCES

- Berends, A. H., Sluys, L. J., & de Borst, R. (1997), Discontinuous modelling of mode-I failure, In M. A. Hendrix, H. Jongedijk, J. G. Rots, & W. J. E. Spanje (Eds.), *Finite Elements in Engineering and Science* (pp. 351–361). Rotterdam: Balkema.
- de Borst, R., Sluys, L. J., Mülhaus, H.-B., & Pamin, J. (1993), Fundamental issues in finite element analyses of localization and deformation, *Engineering Computations*, **10**(5), 99–121.
- Jirásek, M. (1998), *Finite elements with embedded cracks*, Technical Report LSC Internal Report 98/01, École Polytechnique Fédérale de Lausanne, Switzerland.
- Larsson, R. & Runesson, K. (1996), Element-embedded localization band based on regularized displacement discontinuity, *ASCE Journal of Engineering Mechanics*, **122**(5), 402–411.
- Lotfi, H. R. & Shing, P. B. (1995), Embedded representation of fracture in concrete with mixed finite elements, *International Journal for Numerical Methods in Engineering*, **38**(8), 1307–1325.
- Oliver, J. (1996), Modelling strong discontinuities in solid mechanics via strain softening constitutive equations. Part 2: Numerical simulation, *International Journal for Numerical Methods in Engineering*, **39**(21), 3601–3623.

- Oliver, J. & Simo, J. C. (1994), Modelling strong discontinuities by means of strain softening constitutive equations, In H. Mang, N. Bićanić, & R. de Borst (Eds.), *EURO-C 1994 Computer Modelling of Concrete Structures* (pp. 363–372). Swansea: Pineridge Press.
- Pijaudier-Cabot, G. & Bažant, Z. (1987), Nonlocal damage theory, *ASCE Journal of Engineering Mechanics*, **113**(10), 1512–1533.
- Rots, J. G. (1988), *Computational modeling of concrete fracture*, PhD thesis, Delft University of Technology.
- Simo, J. C. & Rifai, M. S. (1990), A class of mixed assumed strain methods and the method of incompatible modes, *International Journal for Numerical Methods in Engineering*, **29**(8), 1595–1638.
- Sluys, L. J. & Berends, A. H. (1998), Discontinuous failure analysis for mode-I and mode-II localization problems, *International Journal of Solids and Structures*, **35**(31–32), 4257–4274.
- Taylor, R. L., Simo, J. C., Zienkiewicz, O. C., & Chan, C. H. (1986), The patch test - a condition for assessing FEM convergence, *International Journal for Numerical Methods in Engineering*, **22**(1), 39–62.
- Wells, G. N. (1999), *Strong Discontinuity Analysis - The classical continuum*, Technical Report LR-TM-99-01, Delft University of Technology, Delft, The Netherlands.